Magnetic resonance imaging biomarkers of exercise-induced improvement of oxidative stress and inflammation in the brain of old high-fat-fed ApoE-/- mice

Erica N. Chirico, Vanessa Di Cataldo, Fabien Chauveau, Alain Geloën, David Patsouris, Benoît Thézé, Cyril Martin, Hubert Vidal, Jennifer Rieusset, Vincent Pialoux, et al.

MRI biomarkers of exercise-induced improvement of oxidative stress and inflammation in the brain of old high fat fed ApoE$^{-/-}$ mice

Erica N Chirico, PhD[*,†,€], Vanessa Di Cataldo, MSc[*], Fabien Chauveau, PhD[‡], Alain Geloën, PhD[*], David Patsouris, PhD[*], Benoît Thézé[¥], Cyril Martin, PhD[†], Hubert Vidal, PhD[*], Jennifer Rieusset, PhD[*], Vincent Pialoux, vincent.pialoux@univ-lyon1.fr, PhD[†,§], and Emmanuelle Canet-Soulas, PhD, MV[*,§]

[*] *University of Lyon, University Lyon 1, Cardiovascular, Metabolism, Diabetes, and Nutrition (CarMeN INSERM U-1060), Faculty of Medicine Hospital Lyon Sud, Oullins, France;*
[†] *University of Lyon, University Lyon 1, Laboratoire Inter-Universitaire de Biologie de la Motricité, (LIBM, EA647), Villeurbanne, France;*
[€] *Cooper Medical School of Rowan University, Department of Biomedical Sciences, Camden, New Jersey, USA*
[‡] *Université de Lyon, Université Lyon 1, Lyon Neuroscience Research Center; CNRS UMR5292; Inserm U1028; Lyon, France*
[¥] *Laboratoire Réparation et Vieillissement, Institut de Radiobiologie Cellulaire et Moléculaire, CEA, Fontenay-aux-Roses, France*

[§]these authors equally contributed to the supervision of this work.

Address for correspondence:
Vincent Pialoux, PhD
Université Claude Bernard Lyon 1
Laboratoire Inter-Universitaire de Biologie de la Motricité (LIBM, EA7424)
27-29 rue du 11 novembre 1918
69622 Villeurbanne cedex, France
tel: (33) 4 72 43 27 42
vincent.pialoux@univ-lyon1.fr

Running title: Exercise improves brain damages in ApoE$^{-/-}$ mice

This is an Accepted Article that has been peer-reviewed and approved for publication in the The Journal of Physiology, but has yet to undergo copy-editing and proof correction. Please cite this article as an 'Accepted Article'; doi: 10.1113/JP271903.

ABSTRACT

Background: Vascular brain lesions, present in advanced atherosclerosis, share pathological hallmarks with peripheral vascular lesions, such as increased inflammation and oxidative stress. Physical activity reduces these peripheral risk factors, but its cerebrovascular effect is less documented, especially by non-invasive imaging.

Objectives: Through a combination of in-vivo and post-mortem techniques, we aimed at characterizing vascular brain damage in old ApoE$^{-/-}$ mice fed a high cholesterol (HC) diet with dietary controlled intake. We then sought to determine the beneficial effects of exercise training on oxidative stress and inflammation in the brain as a treatment option in an aging atherosclerosis mouse model.

Methods: Using in-vivo magnetic resonance imaging (MRI) and biological markers of oxidative stress and inflammation, we evaluated the occurrence of vascular abnormalities in the brain of HC-diet fed ApoE$^{-/-}$ mice over 70 weeks old, its association with local and systemic oxidative stress and inflammation, and whether both can be modulated by exercise.

Results: Exercise training significantly reduced both MRI-detected abnormalities (present in 71% of untrained vs. 14% of trained mice) and oxidative stress (lipid peroxidation: 9.1±1.4 vs. 5.2±0.9 µmol/mg, $p<0.01$) and inflammation (IL-1β: 226.8±27.1 vs. 182.5±21.5 pg/mg, $p<0.05$) in the brain, and the mortality rate. Exercise also decreased peripheral insulin resistance, oxidative stress and inflammation, but significant associations were only seen within brain markers.

Conclusions: Highly localized vascular brain damages are frequent in this aging atherosclerosis model and exercise is able to reduce this outcome and improve lifespan. In-vivo MRI evaluated both the neurovascular damage and the protective effect of exercise.

Key Words: imaging, exercise, inflammation, oxidative stress, atherosclerosis, cerebrovascular, aging

KEY POINTS

- Vascular brain lesions and atherosclerosis are two similar conditions that are overwhelmed by inflammation and oxidative stress.
- Non-invasive imaging in a murine model of atherosclerosis showed vascular brain damage and peripheral inflammation
- In this study, exercise training reduced MRI-detected abnormalities, insulin resistance, and markers of oxidative stress and inflammation in old ApoE$^{-/-}$ mice
- Our results demonstrate the protective effect of exercise on neurovascular damaging in the aging brain of ApoE$^{-/-}$ mice

ABBREVIATION LIST

AOPP, Advanced Oxidation Protein Products; BBB, blood brain barrier; BCA, bicinchoninic acid; CNS, central nervous system; CVD, cardiovascular disease; CS, citrate synthase; FRAP, Ferric reducing antioxidant power; GPX, glutathione peroxidase; HF/HC, high fat/high cholesterol; IL-1β, interleukin-1 beta; MDA: malondialdehyde ; MRI, magnetic resonance imaging; NF-κB, nuclear factor kappa B; NOx, nitric oxide metabolites; O-ApoE-ExT, old $ApoE^{-/-}$ exercise trained; O-ApoE-UT; old $ApoE^{-/-}$ untrained;O-C57- ExT, old C57 mice exercise trained; O-C57-UT, old C57 mice untrained; ROS, reactive oxygen species; SOD, superoxide dismutase; TBA, thiobarbituric acid; TNFα, tumor necrosis factor alpha TPTZ, 2,4,6-Tris(2-pyridyl)-s-triazine; USPIO, ultrasmall iron oxide nanoparticles; VWR, voluntary wheel running; Y- ApoE-UT, young $ApoE^{-/-}$ mice untrained.

INTRODUCTION

Vascular brain lesions develop in a similar manner to that of atherosclerosis as both conditions are overwhelmed by an increased inflammation and oxidative stress. The burden of dementia in the aged population and the recent investigations linking high-risk cardiovascular factors and neurodegenerative diseases incites translational investigations of altered cerebrovascular function in high risk aging patients. Relevant imaging biomarkers are therefore being developed for non-invasive evaluation of lipid-induced peripheral and neurovascular dysfunction, inflammation, and oxidative stress (Briley-Saebo *et al.*, 2012). In the context of aging and disturbed lipid trafficking, the brain is highly susceptible to ROS-induced damage due to its high rate of oxidative metabolism and relatively low levels of antioxidant enzymes (Coyle & Puttfarcken, 1993). It is possible that blood brain barrier (BBB) permeability (Hafezi-Moghadam *et al.*, 2007; Zlokovic, 2008), a cholesterol-rich diet, as well as the macrophage infiltration that is common in atherosclerosis, could also affect the brain vessel function in the aging process (Casserly & Topol, 2004; Saleh *et al.*, 2004). Therefore, risk factors for atherosclerosis could be involved in the development of inflammatory conditions in the brain, and ultimately lead to cerebrovascular ischemia or hemorrhage (Dutta *et al.*, 2012).

Exercise training has been well documented in the amelioration of oxidative stress and inflammation in cardiovascular diseases (CVD) (Lee, 2011). Exercise training is able to reduce oxidative stress by increasing antioxidant capabilities and by maintaining nitric oxide metabolism (Chirico *et al.*, 2012). Exercise training could also be an impetus for an anti-inflammatory environment as aerobic exercise has been associated with lower circulating levels of pro-inflammatory markers (Lesniewski *et al.*, 2011). Exercise is also connected with improvement in general metabolic conditions such as lipid dysfunction and insulin resistance. As shown by Pellegrin et al. (Pellegrin *et al.*, 2009*a*, 2009*b*), the beneficial effects of exercise training on atherosclerosis have been established in young $ApoE^{-/-}$ mice.

In old $ApoE^{-/-}$ under high fat/high cholesterol (HF/HC) diet, acute events such as paralysis, hemiplegia, and sudden death have been observed (unpublished observation) which are highly suggestive of cerebrovascular diseases. We used aortic and brain MRI to further characterize these observations and to highlight the combination of systemic and local effects of exercise in this advanced vascular and metabolic model (Drake *et al.*, 2011). Indeed, a recent review suggested that heart or brain infarcts could be potentiated by a whole-body inflammatory network (Nahrendorf *et al.*, 2015).

We hypothesized that voluntary wheel running (VWR) could ameliorate vascular-induced abnormalities in the brain and decrease inflammation; two conditions that suggest high risk of stroke or other neurovascular complications.

METHODS AND MATERIALS

Ethical Approval

All animal procedures conformed to the European regulation for animal use and this study was approved by the local ethics committee of our institution. All the authors understand the ethical principles under which the Journal of Physiology operates. In addition, the present work complies with the animal ethics checklist of the Journal of Physiology. Finally we have taken all the steps to minimize the animals' pain and suffering for each methodological procedure where animals were involved as detailed below.

In brief, 5 groups of animals were studied: old untrained and exercise trained ApoE$^{-/-}$ mice (C57BL/6 background, Charles-River, France) (O-ApoE-UT; O-ApoE-ExT), young untrained ApoE$^{-/-}$ mice (Y-ApoE-UT), and old untrained and exercise trained C57BL/6 (O-C57-UT; O-C57-ExT). Using *in-vivo* MRI, the ascending aorta and brain were imaged, and contrast agents (iron oxide nanoparticles, P-904 and gadolinium Gd-DOTA, Guerbet, Aulnay-sous-Bois, France) were used to further quantify macrophage infiltration and vascular permeability. At the end of the study, plasma measurements and tissue samples were taken. Total blood cholesterol, insulin, oxidative stress markers (AOPP, MDA, nitrotyrosine), antioxidant markers (catalase, GPX, SOD, FRAP, and NOx), inflammatory markers (TNFα, IL-1β, NF-κB/p65) were measured. Brain samples were stained with standard Hematoxylin Eosin, F4/80 immunostaining for macrophages, and IgG immunostaining for blood brain barrier permeability.

Animals

Male and female ApoE$^{-/-}$ mice (C57BL/6 background, Charles-River, France) were fed a HF/HC diet (Western Diet, 21% fat, 0.15% cholesterol, U8220 version 153, SAFE, Augy, France) starting at 8 weeks of age, and control males and females C57BL/6 mice (Charles-River, France) were fed a normal diet (Standard mice diet, 12% fat, Teklad Global 16% Protein, HARLAN, Gannat, France). All animals were maintained on a 12 hour light-dark cycle and were supplied with food (limited at 20g per week per animal corresponding to 955 kcal per week for ApoE$^{-/-}$ and 688 kcal per week for C57BL/6) and water ad libitum. After careful maintenance of health conditions during one year (Guerbet, Animal Care Unit), 60±1 weeks both old ApoE$^{-/-}$ and C57 mice were randomly divided into 2 activity groups (untrained: UT; exercise trained: ExT). Mice in the exercise trained group (O-ApoE-ExT and O-C57-ExT) were individually housed in cages equipped with a 12.5 cm metal running wheel (HAGEN-61700, Montreal, Canada) and digital magnetic counter (model BC906 Sigma Sport, Neustadt, Germany), while the untrained (O-ApoE-UT and O-C57-UT) group had a standard cage. Males and females young-adult ApoE$^{-/-}$ mice (Y-ApoE-UT; age = 10 weeks) under the same high fat diet (starting at 8 weeks of age; under diet for 14 weeks total) served as age-controls. During the 12 weeks of training, the distance run and the general health (i.e. tumors, skin irritations) of the mice were noted three times a week. The exclusion criterion was overall bad health of the animal (i.e. tumors, skin irritations). A follow-up was performed daily by the technician of the animal facility to evaluate pain on the basis of external physical appearance, weight loss (with respect to food and water ingestion), assessable clinical sign (in particular increase in respiratory frequency), change in behavior (in particular prostration) and non-response to external stimuli.

MRI Protocol

Mice were randomly selected to undergo the imaging protocol. The mice were anesthetized by isoflurane (2% for the induction and 1% to maintain anesthesia) (TEM SEGA, Lormont, France). Cardiac and respiratory rates were monitored throughout the session and body temperature was maintained using a circulating heated water blanket at 37±1°C. MRI acquisitions were performed on a 4.7T Bruker magnet (Ettingen, Germany). The total duration of the MRI protocol was less than 2 hours. The protocol was then repeated 48 hours after the injection of ultrasmall iron oxide nanoparticles (USPIO) (P904, 1 mmol Fe/kg, Guerbet, Aulnay-sous-bois, France) for vessel wall inflammation assessment, followed by the brain imaging acquisition (Figure 1).

Aorta MRI.

For ascending aorta imaging, double cardiac and respiratory gated acquisitions were obtained as previously described (Sigovan *et al.*, 2012) with a homemade gating system developed in Matlab (The MathWorks Inc, Natick, MA). ECG signals were collected via the three electrodes placed on the paws and respiratory signals were collected via a pressure sensor placed on the abdomen.

The ascending and descending aorta were identified using reference axial slices. A bright-blood cine-mode FLASH sequence was used to locate the aortic arch. The reference slices were acquired with a gradient echo (GE) sequence with the following parameters: TR/TE= 1R-R interval/6.7 ms; field of view = 3.8 x 3.8 cm; matrix = 256 x 256; bandwidth = 25 kHz; slice thickness =1.1 mm. The oblique slice was placed perpendicular to the ascending aorta directly above the sinus to avoid flow artifacts.

A black-blood multi-gradient echo sequence was used to image USPIO accumulation using the same slice number and positioning, spatial resolution, partial echo acquisition, and the following parameters: minimum repetition time, 742 milliseconds (achieved by setting the gating system between 3 and 5 RR intervals depending on the animal's heart rate); 4 echoes; band width, 79.3 kHz; and number of averages, 2. The sequence was performed twice with two different TE: 3.1 milliseconds, followed by 4.0 milliseconds. The acquired 8 echo images were interleaved to allow a better sampling of the T2* decay curve.

Brain MRI.

For brain imaging, a birdcage coil of 72-mm inner diameter was used for RF transmission and a surface coil anatomically shaped to the mouse head for reception (Rapid Biomedical, Wurzburg, Germany).

Brain T2-weighted spin-echo images were acquired using a RARE sequence on both axial and coronal planes. T2 RARE and T2* MGE sequence positioned using standard MRI brain anatomical references for careful pre and post-contrast registration were acquired. The RARE sequence was used with the following parameters: TR/TE=4000 /69 ms; field of view = 2 x 2 cm; matrix = 256 x 256; slice thickness = 1 mm; RARE factor = 8, number of slices = 15. The MGE sequence was used with the following parameters: TR/ first TE = 1500 / 2.6 ms; flip angle = 75°, field of view = 2x2 cm; matrix = 256 x 192; slice thickness = 1mm; 12 echoes and echo interval = 3.5 ms, number of slices = 15.

To further characterize the neurovascular lesions, an extended brain MRI protocol was performed in a separate set of old untrained ApoE$^{-/-}$ mice under HF/HC diet (n=10) and old C57BL/6 mice. Neuro-vascular lesions and iron deposits were assessed respectively by baseline T2 and T2* imaging. T2* quantification was obtained using a multi-slice multi-echo gradient echo (MGE) sequence. For BBB permeability assessment, a T1-weighted MGE sequence with identical geometrical parameters was acquired before and 10 minutes after gadolinium chelate (Gd-DOTA, 0.1 mmol/kg, Guerbet, Aulnay-sous-Bois, France) injection with the following parameters: TR/TE= 124/2.8 ms; field of view = 2 x 2 cm; matrix = 256 x 192; slice thickness = 1 mm; number of slices = 15. This was followed by USPIO injection and the 48 hour post-USPIO T2/T2* imaging.

MRI Analysis.

For brain analysis, areas of interest on pre-USPIO T2/T2* images and post-gadolinium T1 images were first visually categorized based on the size of abnormal areas and the number of slices affected. The blinded investigators scored changes in pre- and post- contrast (48 hours post-USPIO) on T2/T2* images and gadolinium leakage on T1-weighted images. Briefly, a score of 1-4 was given for abnormalities seen on pre-contrast images and a score of 1-4 was given for changes seen on post-contrast images (See Table 1 for scoring assessment).

For analysis of the aortic arch, inner and outer vessel wall contours were delineated and vessel wall area calculated. T2* mapping of pre- and post-USPIO series was performed using Matlab (The MathWorks Inc, Natick, MA) on interleaved MSME images. The vessel wall regions of interest (ROIs) were used for the analysis of aortic T2* on both pre- and post-contrast images as described by Sigovan et al(Sigovan *et al.*, 2010).

Dissections

Following the second imaging session, mice were anesthetized by an intraperitoneal injection of pentobarbital (50mg/kg, Dolethal®, Vétoquinol, Lure, France) and blood was collected by cardiac puncture. Mice were sacrificed by exsanguination with a 0.9% NaCl transcardial perfusion for 70 sec. The brain, heart, ascending-descending aorta, liver, and soleus were removed. Sections to be used for biological assays were stored at -80°C until assessment.

Immunohistochemistry

Brain samples were harvested and fixed in a paraformaldehyde solution during 1 hour followed by sucrose for 24 hours and preserved at -80°C until processing. Four successive 15µm thick sections for 3 MRI locations were assessed with standard Hematoxylin Eosin, F4/80 immunostaining for macrophages, and IgG immunostaining for blood brain barrier permeability, as previously described (Wiart et al, 2007). DeadEnd™ Colorimetric TUNEL System kit (PROMEGA, San Luis Obispo, CA, USA) was used to detect DNA fragmentation (apoptosis), F4/80 Antibody (#MF48000, CATALG MEDSYSTEMS, Buckingham, UK) for macrophages and Anti-Mouse IgG (3A9044-2ML, SIGMA) for BBB permeability.

Biological analysis

All tissues were kept frozen and homogenized with a 10% v/w buffer (PBS 1x + 0.5mM EDTA). Homogenates were centrifuged at 4°C for 4 min at 1500g for protein content and MDA analysis, and again at 4°C for 10 min at 12000g for the remaining analyses. Supernatants were frozen at -80°C. Protein concentrations were determined spectrophotometrically (Biophotometre, Eppendorf, Germany) using a bicinchoninic acid (BCA) kit according to instructions (Sigma, St Louis, USA). Protein concentration was

adjusted at 1000µg/mL for brain, heart, and liver and at 100µg/mL for aorta and soleus. All the biological assays were read on a microplate reader (TECAN Infinite M200, Mannedorf, Switzerland).

Markers of metabolism, enzymatic activity, oxidative stress and inflammation

Citrate Synthase

To determine metabolic muscle adaptations to physical activity, skeletal muscle citrate synthase activity was determined using soleus muscle homogenate by the method of Shepherd and Garland(Shepherd & Garland, 1969). Briefly, citrate synthesis rate from acetyl coenzyme A and oxaloacetate was determined according to a coupling reaction between coenzyme A and DTNB (5,5'-Dithiobis(2-nitrobenzoic acid). This coupling reaction was spectrophotometrically measured at 412nm for 45 seconds.

Advanced Oxidation Protein Products (AOPP)

AOPP were determined in plasma, aorta, heart, liver, and brain supernatant using the semi-automated method developed by Witko-Sarsat et al(Witko-Sarsat *et al.*, 1996), as previously described (Pialoux *et al.*, 2009*b*). Briefly, AOPP were measured by spectrometry and were calibrated with a chloramine-T solution that absorbs at 340 nm in the presence of potassium iodide. The absorbance of the reaction was immediately read at 340 nm on the microplate reader against a blank containing 200 µl of PBS. AOPP activity was expressed as micromoles per liter of chloramines-T equivalents.

Catalase

Catalase activity in the plasma, heart, and brain were determined by the method of Johansson and Borg (Johansson & Borg, 1988), using hydrogen peroxide (H_2O_2) as a substrate, and formaldehyde as standard. Catalase activity was determined by the formation rate of formaldehyde, read at 540 nm during 20min, induced by the reaction of methanol and H_2O_2 using catalase as enzyme.

Ferric Reducing Antioxidant Power (FRAP)

Plasma FRAP was measured by spectrophotometry using the method of Benzie and Strain(Benzie & Strain, 1996). Briefly, FRAP concentration was calculated using an aqueous solution of a known Fe^{2+} concentration ($FeSO_4$-$7H_2O$) as the standard. Plasma was mixed with a FRAP working solution at 37°C, containing buffer acetate, 2,4,6-Tris(2-pyridyl)-s-triazine (TPTZ), and ferric choloride ($FeCl_3$-$6H_2O$). The Fe^{2+}-TPZT complex subsequently formed was read at 593 nm after 4 min

Glutathione Peroxidase (GPX)

GPX in the plasma, heart, liver, and brain was determined by the modified method of Paglia and Valentine(Paglia & Valentine, 1967), using hydrogen peroxide (H_2O_2) as a substrate. GPX was determined by the rate of oxidation of NADPH to $NADP^+$ after addition of glutathione reductase (GR), reduced glutathione (GSH), and NADPH. NADPH extinction was read at 340nm during 5 min.

Malondialdehyde (MDA)

Although MDA assay shows methodological limitations(Lefèvre *et al.*, 1998), it is the most common lipid peroxidation marker and it is still a widely used marker of oxidative stress. Concentrations of plasma, heart, liver and brain MDA were determined as thiobarbituric acid (TBA) reactive substances by a modified method of Ohkawa et al(Ohkawa *et al.*, 1979)(1979), as previously described(Pialoux *et al.*, 2009*a*). The pink chromogen of the complex TBA-MDA formed after 1h at 100°C was extracted with n-butanol, and its absorbance was measured at 532 nm by spectrophotometry. MDA concentration was calculated using 1,1,3,3-tetraethoxypropane as standard.

Nitrite and Nitrate (NOx)

The end-products of endothelium nitric oxide, nitrites and nitrates, were measured in the plasma, based on methods previously described(Misko *et al.*, 1993). The sum of nitrite and nitrate in the plasma (NOx) is considered an index of nitric oxide production(Hebbel *et al.*, 1982). Briefly, the fluorometric quantification of nitrite/nitrate is based upon the reaction of nitrite with 2,3-diaminonaphthalene to form the fluorescent product, 1-(H)-naphthotriazole and read at 450nm after excitation at 365nm. Nitrates are converted to nitrite by nitrate reductase.

Nitrotyrosine

Concentrations of plasma nitrotyrosine, as end product of protein nitration by $ONOO^{\cdot-}$, were measured by a competitive enzyme-linked immunosorbent assay as previously described(Galiñanes & Matata, 2002) using pre-coated nitrated bovine serum albumin microplates and subsequent incubations and washings of anti-nitrotyrosine and anti-rabbit IgG – HRP-conjugate. Concentration of nitrotyrosine was then calculated using nitrated bovin serum albumin as standard.

Superoxide dismutase (SOD)

The quantitative determination of the SOD activity was performed on the plasma, aorta, heart, liver, and brain using the Beauchamps and Fridovich's method(Beauchamp & Fridovich, 1971), slightly modified by Oberley and Spitz(Oberley & Spitz, 1985). SOD activity was determined by the degree of inhibition of the reaction between superoxide radicals, produced by a hypoxanthine-xanthine oxidase system, and nitroblue tetrazolium. The formazan blue subsequently formed was read at 560nm during 5 min.

Cholesterol and metabolic measurements

Total blood cholesterol was assessed using Amplex Red Cholesterol Assay Kit as instructed by Invitrogen (Carlsbad, CA). One week before MRI, intraperitoneal insulin tolerance test (IPITT) was performed on 6h-fasted mice. Mice were injected intraperitoneally with 0.75mU/g body weight of insulin. Blood was taken by tail puncture immediately before and at 15, 30, 45 and 60 min points after injection for measurement of blood glucose.

All reagents used for biochemical assays were purchased from Sigma Aldrich.

Inflammatory Markers

TNFα (BD Biosciences, San Jose, CA) and IL-1β (RayBiotech, Inc, Norcross, GA) were assessed in plasma, aorta, and brain supernatant, and IL-4 (Abcam, Cambridge, UK) in brain supernatant using a commercially available mouse enzyme-linked immunosorbent assay kit, according to manufacturer instructions. NF-κB/p65 activity (IMGENEX, San Diego, CA) was assessed in plasma according to manufacturer instructions.

Statistics

Statistical analyses were conducted using Statistica (version 8.0, Statsoft, Tulsa, OK, USA). Results are presented as mean ± SD. For each parameter, a minimum of 7 mice per group was used. Statistical comparisons between 5 groups (O-ApoE-UT, O-ApoE-ExT, Y-ApoE-UT, O-C57-UT, O-C57-ExT) were performed by one-way analysis of variance followed by Bonferroni post hoc test. Pearson's coefficient correlations were used to determine the associations between plasma markers, brain markers, and distance run. Logrank test was used for survival curve analysis. Statistical significance was determined by a P value of less than 0.05. All the animal that did not complete the study were excluded from all the analyses done except for the calculation of the survival rate.

RESULTS

Animal characteristics and general effects of exercise

91 old ApoE$^{-/-}$, 20 young-adult ApoE$^{-/-}$ and 16 old C57BL/6 (O-C57) mice were originally included in the protocol. These animals were vulnerable to cerebrovascular disease, especially in the older cohorts, and a number of animals died prior to any biological assessment. The majority of these animals died spontaneously; however 7 mice died after signs of mono- or hemi-plegia (all being old ApoE$^{-/-}$, representing 13% of all deaths of this group), a possible symptom of cerebrovascular disease. Of the mice that died during the protocol, 29 were in the O-ApoE-UT group, 10 were in the O-ApoE-ExT group (Figure 2), 1 in the O-C57-UT and 1 in the O-C57-ExT group. An additional 6 mice died during insulin resistance test or MRI, and 3 mice were excluded at autopsy because of large tumors. After the induction and training period, 43 old ApoE$^{-/-}$ mice (19 O-ApoE-UT: 72.4±2.4 weeks and 24 O-ApoE- ExT: 71.8±1.9 weeks) and 20 young-adult mice (Y-ApoE-UT: 20±0 weeks) were used for biological assessment (Table 2). O-ApoE-ExT mice ran 17.8±15.3 km/week whereas the O-C57-ExT mice ran 16.2±8.8 km/week. The training effect was supported by higher CS activity in the soleus of both O-ApoE-ExT and O-C57-ExT mice compared to corresponding UT mice (see Table 2). Despite higher plasma cholesterol levels in all ApoE$^{-/-}$ compared with old C57 mice (independently of training), Y-ApoE-UT mice had higher insulin sensitivity than O-ApoE-UT (Table 3). The training effect was also evident on both insulin sensitivity and plasma cholesterol levels in the O-ApoE-ExT versus the corresponding untrained mice (see Table 2). Importantly, the O-ApoE-ExT mice had a significant higher survival rate compared to the O-ApoE-UT mice (77 vs. 49%, p=0.03; Figure 2), Exercise training was therefore able to decrease the mortality rate of the old ApoE$^{-/-}$ mice. Both O-C57-UT and O-C57-ExT had a survival rate of 87%, which was significantly higher than the old ApoE$^{-/-}$ mice confirming the pathological state of our old ApoE$^{-/-}$ mice.

Presence of multiple neurovascular lesions in old sedentary ApoE$^{-/-}$ mice under HF/HC diet

As observed by *in vivo* MRI and histology, there were significant abnormalities in the brain vasculature of O-ApoE-UT mice (Figure 3) whereas O-C57-UT did not show such

abnormalities as indicated by significantly lower scoring between old O-ApoE-UT and O-C57-UT for both post-USPIO T2 and post-gadolinium T1 images (Figure 3). On pre-contrast images, several dark areas on T2 images and T2* images indicated iron accumulation in a large number of O-ApoE-UT mice at the same periventricular location (71% of O-ApoE-UT vs. 0% for O-C57-UT). Post-gadolinium T1 images indicated the presence of periventricular blood brain barrier leakage and endothelial permeability in O-ApoE-UT mice (Gadolinium score of 2.7±0.80 for O-C57-UT mice vs. 1.42±0.23 for O-C57-UT, $p<0.05$) (Figure 3). Comparing the pre- to post-USPIO T2 images (Figure 3), it was evident that there was also an accumulation of iron oxide nanoparticles. Because circulating iron oxide nanoparticles would have been cleared from the circulation, this suggests the presence of macrophages and phagocytic activity in the same area. These signs of neuro-inflammation observed on both post-USPIO T2* and T2 images were confirmed by histology (Figure 4). Disorganized brain parenchyma was seen in the middle ventral zone, but was not related to an active apoptotic process (TUNEL negative on immunohistochemistry, data not shown). There was also an anatomical correspondence between this abnormal area in both T2/T2* images and post-gadolinium T1 images, which were histologically confirmed respectively by positive staining for IgG and F4/80. This would indicate BBB leakage (endothelial permeability). There was also some evidence of vesicular aggregates, which could indicate foam cell development (data not shown).

Brain MRI in trained versus untrained old ApoE$^{-/-}$ mice

There were significantly more abnormalities in the brain vasculature of O-ApoE-UT (n=7; 71% of mice) compared to O-ApoE-ExT, (n=7, 14% of mice). Comparing the pre-USPIO images (respective scores, 1.71±0.19 *vs.* 1.29±0.19; $p=0.12$) to post-USPIO images, there was more USPIO accumulation in O-ApoE-UT mice (vs. O-ApoE-ExT) suggesting phagocytic activity and inflammation (Figure 3 and 4) as indicated by the significantly higher post-USPIO T2* score in O-ApoE-UT mice compared to O-ApoE-ExT mice (2.92±0.49 *vs.* 1.69±0.44; $p<0.05$).

Old ApoE$^{-/-}$ expressed higher brain oxidative stress and inflammation than old C57 and young ApoE$^{-/-}$

MDA, AOPP, Il-1β, and TNFα were significantly lower and FRAP significantly higher in O-C57-UT than in O-ApoE-UT mice ($p<0.01$) confirming the brain pathological state of our old ApoE$^{-/-}$ mice (Table 4). SOD and GPX were not different between O-C57-UT and O-ApoE-UT (Table 4). Brain concentrations of oxidative stress marker MDA and pro-inflammatory markers, TNFα and IL-1β, were significantly higher in both O-ApoE-UT and O-ApoE-ExT compared to Y-ApoE-UT, ($p<0.01$). On the contrary, SOD and GPX (see Table 4) and IL-4 O-ApoE-UT: 2.34±0.83 pg/mg vs. Y-ApoE-UT: 5.04±3.26 pg/mg; $p<0.05$) were decreased with age in ApoE$^{-/-}$ mice.

Exercise-induced changes in markers of oxidative stress and inflammation in the brain of old ApoE$^{-/-}$ mice (Table 3).

In the brain, MDA and AOPP were decreased in response to exercise training ($p<0.01$ and $p<0.05$ respectively). Moreover, there was an increase in brain catalase ($p<0.05$), and a decrease in Il-1β and TNFα in O-ApoE-ExT compared to O-ApoE-UT mice ($p<0.05$). Brain concentrations of IL-4 were significantly higher in in O-ApoE-ExT compared to O-ApoE-UT mice (5.70±3.87 vs. 2.34±0.83 pg/mg for O-ApoE-ExT and O-ApoE-UT respectively; $p<0.05$). FRAP, GPX and SOD were not significantly affected by exercise in old ApoE$^{-/-}$ mice.

Aorta MRI and biological vessel wall response

O-ApoE-UT mice had a larger vessel wall area than the Y-ApoE-UT (4.02±0.22 vs. 2.66±0.03 mm^2; $p<0.01$). In the O-ApoE-ExT mice, vessel wall area was reduced compared to O-ApoE-UT mice (see Figure 5). Concerning T2* measurements, both pre and post-USPIO values in O-ApoE-UT mice were lower than in Y-ApoE-UT mice, confirming respectively more complex plaque composition and more inflammatory activity (Mihai *et al.*, 2011). The O-ApoE-Ext mice had an increase in pre-USPIO T2* measurement compared to O-ApoE-UT mice, suggesting a less complex plaque composition (see Figure 5). Post-USPIO T2* was lower than pre-contrast values for all the groups, indicating the presence of iron particles and phagocytic activity in the vessel wall. In the aorta, both O-ApoE-ExT and O-ApoE-UT mice had more TNFα, IL-1β, and AOPP, than Y-ApoE-UT mice whereas only O-ApoE-UT had more SOD than Y-ApoE-UT mice. O-ApoE-UT mice had more TNFα, IL-1β, AOPP and SOD in the aorta than O-ApoE-ExtT (see Table 5) ($p<0.05$). AOPP, Il-1β, and TNFα in the aorta were much lower in old C57 than in old $ApoE^{-/-}$ independent of exercise training ($p<0.01$) which strengthens the atherosclerotic phenotype seen in the aorta of old $ApoE^{-/-}$ mice.

Heart markers

Heart concentrations of AOPP were higher in O-ApoE-UT compared to Y-ApoE-UT mice. O-ApoE-UT mice had lower GPX and SOD than Y-ApoE-UT mice. AOPP and antioxidant enzymes (SOD, GPX, and catalase) were higher in old C57 compared to old $ApoE^{-/-}$ (Table 6). O-ApoE-ExT mice had higher levels of SOD and lower AOPP than O-ApoE-UT mice (see Table 6).

Liver markers

Liver concentrations of AOPP and MDA were higher in O-ApoE-UT compared to both Y-ApoE-UT and O-C57-UT mice whereas liver GPX activity was lower in O-ApoE-UT than in Y-ApoE-UT. In addition, O-ApoE-ExT mice had higher levels of SOD and GPX and lower AOPP and MDA than O-ApoE-UT mice (see Table 6).

Systemic oxidative stress and inflammation is higher in old $ApoE^{-/-}$ compared to old C57

Nitrotyrosine, and AOPP were higher ($p<0.05$) whereas NOx ($p<0.05$) was lower in old $ApoE^{-/-}$ compared with old C57 independently of training (Table 7). GPX was higher in O-C57-ExT than in O-ApoE-UT ($p<0.01$).

Exercise-induced changes in systemic oxidative stress and inflammation

Plasma MDA decreased in response to exercise training in the old $ApoE^{-/-}$ mice (23.3±1.8 vs. 17.9±1.7 µmol/L for O-ApoE-UT and O-ApoE-ExT respectively, $p<0.05$) whereas AOPP showed a trend to increase ($p=0.09$, Table 7). The plasma volume collected from for O-C57-ExT and O-C57-U mice was insufficient to allow plasma MDA analysis for these 2 groups of mice. Antioxidant markers NOx and SOD were higher in O-ApoE-ExT than in O-ApoE-UT (respectively $p<0.05$ and $p=0.11$, Table 7). Plasma AOPP were higher in O-ApoE-UT mice compared to Y-ApoE-UT ($p<0.01$, see Table 7) while MDA were lower (23.3±1.8 vs. 8.8±0.6 µmol/L for O-ApoE-UT and Y-ApoE-UT respectively, $p<0.01$). Pro-inflammatory markers, TNFα and IL-1β were also significantly different in old $ApoE^{-/-}$mice compared to young-adult mice ($p<0.001$). Interestingly, NOx, SOD and GPX were improved in the trained old C57 (vs untrained). On the contrary, in $ApoE^{-/-}$ mice under HF/HC, NFkB was not significantly affected by age or exercise training (Y-ApoE-ExT: 97.4±13.6 pg/mL; O-ApoE-UT: 102.3±15.6 pg/mL; O-ApoE-ExT: 84.1±12.2 pg/mL).

Correlations

Inflammation and oxidative stress markers were correlated within the brain (see Table 8). However, none of the brain markers were correlated with corresponding plasma (see Table 9), aorta, heart, or liver markers.

DISCUSSION

Vascular brain lesions share similar pathological features with atherosclerosis, such as increased inflammation and oxidative stress (Dutta *et al.*, 2012). In this study, we found that compared to age-matched C57 under normal diet and to young ApoE$^{-/-}$, old ApoE$^{-/-}$ mice under high fat high cholesterol diet exhibited increases in brain abnormalities and BBB permeability in specific periventricular areas as confirmed by both MRI and histology. These results were associated with an increase of both inflammation and oxidative stress markers in the brain in the old ApoE$^{-/-}$ mice. All these phenotypic changes are likely responsible for the low survival (49% over 12 weeks) of ApoE$^{-/-}$ sedentary mice compared with C57BL6 (87%) which confirms the literature (Rowlatt *et al.*, 1976; Blackwell *et al.*, 1995; Moghadasian *et al.*, 2001). More importantly, we found that in aging ApoE$^{-/-}$ mice, exercise training, possibly via its oxidative stress and inflammation lowering capabilities, reduced brain macrophage infiltration, limited inflammation and oxidative stress in the brain, and improved metabolic conditions, thereby improving health status and life expectancy.

Inflammation and oxidative stress in old ApoE$^{-/-}$ mice under high fat high cholesterol diet

Oxidative stress in the cerebral vasculature plays a critical role in the pathogenesis of ischemic brain injury (such as a compromised BBB (Hafezi-Moghadam *et al.*, 2007; ElAli *et al.*, 2011) and macrophage accumulation), especially in the aged ApoE$^{-/-}$ mouse model (Coyle & Puttfarcken, 1993). BBB disruption, as measured here *in vivo* by the extent of gadolinium leakage in T1-weighted MRI, is a sign of endothelial permeability (Gloor *et al.*, 2001). During conditions of inflammation, macrophages are able to cross the BBB and infiltrate the CNS parenchyma as suggested by iron oxide nanoparticle-enhanced MRI in stroke patients and models (Nighoghossian *et al.*, 2007; Wiart et al. 2007). In our study, the location of gadolinium leakage corresponded anatomically with the presence of macrophages detected *in vivo* after injection of iron nanoparticles by T2/T2*-weighted MRI and post mortem by histology. The iron accumulation observed on pre-contrast T2* in some old mice may have resulted from repeated micro-hemorrhage, and could possibly explain the observed symptoms of hemi- and monoplegia. It should be acknowledge that noninvasive MRI with nanoparticles or gadolinium agents has previously demonstrated effectiveness in evaluating endothelial permeability, or in mapping atherosclerotic vascular territories in ApoE$^{-/-}$ mice fed with high fat diet (Phinikaridou *et al.*, 2012), as well as in other experimental cerebral models (Wiart *et al.*, 2007; Koffie *et al.*, 2011). We have shown that combined brain and vascular inflammation imaging provide biomarkers of central and vascular metabolic and inflammation dysfunctions in this mouse model. In addition, our study is also the first to demonstrate that such imaging was sufficiently sensitive to detect beneficial effect of exercise training.

In this advanced atherosclerosis model, our study confirms the presence of multi-organ inflammation as previously described in CVD (Nahrendorf *et al.*, 2015), as well as oxidative stress. Elevated marker concentrations were found in the aortic wall, brain, heart, and liver. As they were not correlated, it can be hypothesized that local microenvironments drive

specific pathologic consequences. Indeed, brain inflammation was far more pronounced and was associated with severe functional impairments in periventricular areas, i.e. BBB damage and high phagocytic activity in the untrained ApoE$^{-/-}$ mice. Also, the observation of motor deficiency cases and the increased mortality rate in the untrained group are likely driven by these brain abnormalities shown by MRI. Local vicious circles of inflammation may be further nourished by systemic and distant inflammatory foci.

Effects of exercise training

We also show that even in an advanced atherosclerotic mouse model, VWR was able to reduce risk factors for atherosclerosis and cerebrovascular damages by altering macrophage accumulation, oxidative stress, inflammation, and metabolic parameters. Our mice ran 17.8 km/week similarly to the age-matched C57 (16.2 km/week). These weekly distance are also close to those reported by Soto et al (Soto *et al.*, 2015) (23 km/weeks) that used voluntary wheel running in ApoE$^{-/-}$ mice under a standard diet. These distances are much greater than forced treadmill running protocol which is usually comprised between 4 and 6 km per week. As mice are naturally active, VWR provides a stress-free way to exercise, as opposed to forced treadmill training and swimming which may induce a stress response (Moraska *et al.*, 2000). The total running distance with VWR is often superior to forced exercise, and it has been shown to produce cardiovascular adaptations such as heart and left ventricular hypertrophy, and an increase in muscle oxidative capacity (Aufradet *et al.*, 2012). Although the distance run by the mice in this study was lower than healthy C57 mice (Aufradet *et al.*, 2012), it was sufficient to increase muscle citrate synthase activity, a commonly used marker of an adaptation to habitual exercise (Sexton, 1995). VWR was also shown to be of moderate intensity rather than high intensity as it could be seen in treadmill running.

In addition, VWR, regardless of exact distance, was able to induce a positive stimulus and reduced overall mortality compared to sedentary old animals. This is consistent with previous reports that physical inactivity is an independent predictor of mortality in animals (Laufs *et al.*, 2005) and humans (Szostak & Laurant, 2011), whereas physical fitness is associated with preserved brain health (Weuve *et al.*, 2004; Podewils *et al.*, 2005). A previous study found that VWR was sufficient to extend survival and decrease neuronal damage after a short episode of forebrain ischemia (Stummer *et al.*, 1994). In treadmill trained rats, induced brain injury was also less severe as a consequence of improved brain integrity (Ding *et al.*, 2006), and BBB function (Davis *et al.*, 2007). On brain MRI, old trained ApoE$^{-/-}$ mice showed a significantly decreased score of BBB leakage at the locations where this dysfunction was observed in their untrained counterparts. Beneficial effects of exercise training on neurovascular damages or brain via increased pericyte number has been recently reported in ApoE$^{-/-}$ (Soto *et al.*, 2015). These adaptive effects may be the result of repetitive cerebrovascular shear stress induced by each bout of running training and long-term increase in cerebral blood flow, both leading to decrease in oxidative stress and endothelial dysfunction activation in brain (Viboolvorakul & Patumraj, 2014). In this context, exercise training was also shown to restore the impaired NOS-dependent responses of cerebral arterioles in diabetic rats (Mayhan *et al.*, 2011) and the impaired dilator responses of cerebral arterioles and in rats submitted to chronic exposure to nicotine (Mayhan *et al.*, 2010). In both studies, beneficial effects of exercise were associated with SOD increase and subsequent superoxide content decrease. In our study, although we did not find any effect of exercise on the brain SOD and GPX activities, lipid peroxidation was reduced suggesting that ROS content may be reduced. Since antioxidant therapies have been shown to reduce infarct volume and neurologic impairment in different murine models of ischemic stroke (Majid,

2014), it could be hypothesized that the beneficial effect of exercise that we observed in the brain could partially be drawn from decrease in oxidative stress.
In contrast to a recent study by Soto et al (2015), our mice were under a HC/HF diet and were indeed more pathologic than under a chow diet, as confirmed by the mortality of our old ApoE$^{-/-}$ mice (65% in 12 weeks at 70 weeks) compared with the 18-24 months old mice used by Soto et al (2015) that suggests a longer life expectancy. The HF/HC diet in ApoE$^{-/-}$ mice was previously shown to induce major changes at the level of the neurovascular unit (Badaut *et al.*, 2012). Interestingly, this change included lipid droplet accumulation and BBB leakage at the same location as in our old ApoE$^{-/-}$ mice.
Additionally, exercise training reduced pro-inflammatory markers which could be due to a concomitant increase in anti-inflammatory cascades(Pedersen, 2006; Szostak & Laurant, 2011) as we found for brain IL-4. Exercise was also shown to reduce brain IL-1β in a mouse model of Alzheimer Disease(Nichol *et al.*, 2008) and brain inflammation in response to stroke(Ding *et al.*, 2005), possibly through an increase in anti-inflammatory pathways at the level of the neurovascular unit.

Better brain health has been shown to be related to systemic improvement of cardiovascular health, lipid-cholesterol balance, and inflammation(Pedersen, 2006). Here, beyond its effects on the brain, exercise training was able to improve the overall effects of atherosclerosis in the old ApoE$^{-/-}$. More specifically, O-ApoE-ExT expressed lower oxidative stress and inflammation in aorta than their sedentary counterparts. MRI revealed a decrease in vessel wall size in the mice that ran compared to sedentary mice, in agreement with others (Shimada et al., 2007; Pellegrin et al., 2009b; Kadoglou et al., 2011). In a study by Pellegrin et al (Pellegrin et al., 2009b), swim-trained ApoE$^{-/-}$ mice showed a decrease in macrophage accumulation, along with an increase in smooth muscle cell content suggesting a more stable plaque. Exercise trained mice had higher T2* values suggesting a more stable plaque (Sigovan *et al.*, 2010). Nevertheless, in future studies, measurement of biological markers of plaque stability in aortic tissue, such as metalloproteinases activity, should confirm this hypothesis.

In old ApoE$^{-/-}$ mice, training decreased plasma, heart, and liver oxidative stress markers, in addition to brain and aorta, suggesting that exercise may have a whole-body effect on oxidative stress in this model.

Compared to old ApoE$^{-/-}$ mice, oxidative stress is very low in the old C57 mice (between 5 and 10 times lower than old ApoE$^{-/-}$ mice in the different organs). This suggests that C57 at the age of 70 weeks might have maintained their pro/antioxidant balance. We also think that further reduction of oxidative stress could be more detrimental than beneficial. Indeed, ROS and lipid peroxidation end-products (like MDA) also have a role in the regulation and modulation antioxidant cell signaling and gene expression, and a decrease of such products, when they are not in excess, may limit physiological adaptations (Niki, 2009).

Finally, although we report clear differences between O-ApoE-ExT and O-ApoE-UT regarding brain and aorta that suggest beneficial effects of exercise training, a longitudinal follow-up of aortic and brain inflammation by MRI may be one of the perspectives of this study to confirm our results.

In conclusion, we found that CVD risk factors, which involve chronic systemic oxidative stress and inflammation, are associated with neuro-vascular lesions in old ApoE$^{-/-}$ mice at specific “at-risk” locations. All together our results demonstrate that 12 weeks of moderate

intensity physical activity was able to improve survival in aged ApoE$^{-/-}$ mice and decrease the extent of the neuro-vascular damages present in this dyslipidemic aged mouse model. This voluntary wheel running protocol decreased both brain disorders (BBB leakage and macrophage accumulation) and aortic plaque size, and increased aortic plaque stabilization. The decrease in oxidative stress and inflammation directly at the brain level as a result of exercise training could be responsible for the neuro-protective effect and the reduced prevalence of lesions. Taken together these results demonstrate the benefits of exercise training in a model of atherosclerosis. Finally, on the basis of this study, non-invasive imaging such as MRI appears to be an essential tool i) to evaluate neurovascular risk in the brain of atherosclerotic patients and ii) to measure therapeutic intervention such as physical exercise with both a site-specific location and combined imaging biomarkers to evaluate exercise effect on blood brain barrier integrity and decrease of neuro-inflammation. More advanced hybrid molecular imaging techniques such as PET/MRI and targeted nanoparticles(Briley-Saebo *et al.*, 2012) may provide longitudinal follow-up and new therapeutic options for these complex high risk cardiovascular profiles.

Acknowledgements: To Guerbet for supplying the contrast agent and the old ApoE$^{-/-}$ mice. To Radu Bolbos and Jean-Baptiste Langlois at CERMEP imaging platform for brain acquisitions. To Andrew Fowler and Monica Sigovan for Matlab developments for MRI analysis. To Charles Vilallonga for brain immo-histochemistry analyses.

Competing interest: The authors declare that they have no conflict of interest.

Author contributions:

ENC, VP and ECS designed the study;
ENC, VDC, FC, AG, DP, BT, JR, VP and ECS analyzed the data;
ENC, VDC, FC, AG, DP, BT, CM, JR, HV, VP and ECS interpreted the data;
ENC, VP and ECS drafted the manuscript;
ENC, VDC, FC, AG, DP, CM, JR, HV, VP and ECS revised the manuscript critically for important intellectual content;
ENC, VDC, FC, AG, DP, CM, JR, HV, VP and ECS approved the final version of the manuscript submitted, agree to be accountable for all aspects of the work in ensuring that questions related to the accuracy or integrity of any part of the work are appropriately investigated and resolved, and all persons designated as authors qualify for authorship, and all those who qualify for authorship are listed.

Funding Sources: This study was supported by the Institut Universitaire de France and the French Ministry of Research for PhD students.

TRANSLATIONAL PERSPECTIVE

- Vascular brain lesions share pathological hallmarks with atherosclerosis, such as increased inflammation and oxidative stress.
- We show that an aging model of atherosclerosis (old ApoE$^{-/-}$ mice under high fat high cholesterol diet) presented vascular brain damage and that these neurovascular disorders were associated with peripheral inflammation. Interestingly, exercise training was able to reduce these pathological outcomes.
- Our finding suggest that non-invasive imaging could be used to evaluate neurovascular risk in atherosclerosis and that regular physical activity may reduce these risks

REFERENCES

Aufradet E, Bessaad A, Alsaid H, Schäfer F, Sigovan M, De Souza G, Chirico E, Martin C & Canet-Soulas E (2012). In vivo cardiac anatomical and functional effects of wheel running in mice by magnetic resonance imaging. *Exp Biol Med (Maywood)* **237,** 263–270.

Badaut J, Copin J-C, Fukuda AM, Gasche Y, Schaller K & Silva RF da (2012). Increase of arginase activity in old apolipoprotein-E deficient mice under Western diet associated with changes in neurovascular unit. *Journal of Neuroinflammation* **9,** 132.

Beauchamp C & Fridovich I (1971). Superoxide dismutase: improved assays and an assay applicable to acrylamide gels. *Anal Biochem* **44,** 276–287.

Benzie IF & Strain JJ (1996). The ferric reducing ability of plasma (FRAP) as a measure of "antioxidant power": the FRAP assay. *Anal Biochem* **239,** 70–76.

Blackwell BN, Bucci TJ, Hart RW & Turturro A (1995). Longevity, body weight, and neoplasia in ad libitum-fed and diet-restricted C57BL6 mice fed NIH-31 open formula diet. *Toxicol Pathol* **23,** 570–582.

Briley-Saebo KC, Nguyen TH, Saeboe AM, Cho Y-S, Ryu SK, Volkova ER, Volkava E, Dickson S, Leibundgut G, Wiesner P, Weisner P, Green S, Casanada F, Miller YI, Shaw W, Witztum JL, Fayad ZA & Tsimikas S (2012). In vivo detection of oxidation-specific epitopes in atherosclerotic lesions using biocompatible manganese molecular magnetic imaging probes. *J Am Coll Cardiol* **59,** 616–626.

Casserly I & Topol EJ (2004). Convergence of atherosclerosis and Alzheimer's disease: inflammation, cholesterol, and misfolded proteins. *The Lancet* **363,** 1139–1146.

Chirico EN, Martin C, Faes C, Feasson L, Oyonno-Engelle S, Aufradet E, Dubouchaud H, Francina A, Canet-Soulas E, Thiriet P, Messonnier L & Pialoux V (2012). Exercise training blunts oxidative stress in sickle cell trait carriers. *Journal of Applied Physiology*. **112**, 1445-1453.

Coyle J & Puttfarcken P (1993). Oxidative stress, glutamate, and neurodegenerative disorders. *Science* **262,** 689–695.

Davis W, Mahale S, Carranza A, Cox B, Hayes K, Jimenez D & Ding Y (2007). Exercise pre-conditioning ameliorates blood-brain barrier dysfunction in stroke by enhancing basal lamina. *Neurol Res* **29,** 382–387.

Ding Y-H, Ding Y, Li J, Bessert DA & Rafols JA (2006). Exercise pre-conditioning strengthens brain microvascular integrity in a rat stroke model. *Neurol Res* **28,** 184–189.

Ding Y-H, Young CN, Luan X, Li J, Rafols JA, Clark JC, McAllister JP 2nd & Ding Y (2005). Exercise preconditioning ameliorates inflammatory injury in ischemic rats during reperfusion. *Acta Neuropathol* **109,** 237–246.

Drake C et al. (2011). Brain inflammation is induced by co-morbidities and risk factors for stroke. *Brain Behav Immun* **25,** 1113–1122.

Dutta P et al. (2012). Myocardial infarction accelerates atherosclerosis. *Nature* **487**:325-329.

ElAli A, Doeppner TR, Zechariah A & Hermann DM (2011). Increased Blood–Brain Barrier Permeability and Brain Edema After Focal Cerebral Ischemia Induced by Hyperlipidemia Role of Lipid Peroxidation and Calpain-1/2, Matrix Metalloproteinase-2/9, and RhoA Overactivation. *Stroke* **42,** 3238–3244.

Galiñanes M & Matata BM (2002). Protein nitration is predominantly mediated by a peroxynitrite-dependent pathway in cultured human leucocytes. *Biochem J* **367,** 467–473.

Gloor SM, Wachtel M, Bolliger MF, Ishihara H, Landmann R & Frei K (2001). Molecular and cellular permeability control at the blood-brain barrier. *Brain Res Brain Res Rev* **36,** 258–264.

Hafezi-Moghadam A, Thomas KL & Wagner DD (2007). ApoE deficiency leads to a progressive age-dependent blood-brain barrier leakage. *Am J Physiol Cell Physiol* **292,** C1256–C1262.

Hebbel RP, Eaton JW, Balasingam M & Steinberg MH (1982). Spontaneous oxygen radical generation by sickle erythrocytes. *J Clin Invest* **70,** 1253–1259.

Johansson LH & Borg LA (1988). A spectrophotometric method for determination of catalase activity in small tissue samples. *Anal Biochem* **174,** 331–336.

Kadoglou NPE, Kostomitsopoulos N, Kapelouzou A, Moustardas P, Katsimpoulas M, Giagini A, Dede E, Boudoulas H, Konstantinides S, Karayannacos PE & Liapis CD (2011). Effects of exercise training on the severity and composition of atherosclerotic plaque in apoE-deficient mice. *J Vasc Res* **48,** 347–356.

Koffie RM, Farrar CT, Saidi L-J, William CM, Hyman BT & Spires-Jones TL (2011). Nanoparticles enhance brain delivery of blood-brain barrier-impermeable probes for in vivo optical and magnetic resonance imaging. *Proc Natl Acad Sci USA* **108,** 18837–18842.

Laufs U, Wassmann S, Czech T, Münzel T, Eisenhauer M, Böhm M & Nickenig G (2005). Physical inactivity increases oxidative stress, endothelial dysfunction, and atherosclerosis. *Arterioscler Thromb Vasc Biol* **25,** 809–814.

Lee S (2011). Effects of interventions on oxidative stress and inflammation of cardiovascular diseases. *World Journal of Cardiology* **3,** 18.

Lefèvre G, Beljean-Leymarie M, Beyerle F, Bonnefont-Rousselot D, Cristol JP, Thérond P & Torreilles J (1998). [Evaluation of lipid peroxidation by measuring thiobarbituric acid reactive substances]. *Ann Biol Clin (Paris)* **56,** 305–319.

Lesniewski LA, Durrant JR, Connell ML, Henson GD, Black AD, Donato AJ & Seals DR (2011). Aerobic exercise reverses arterial inflammation with aging in mice. *Am J Physiol Heart Circ Physiol* **301,** H1025-1032.

Majid A (2014). Neuroprotection in Stroke: Past, Present, and Future. *International Scholarly Research Notices* **2014,** e515716.

Maxwell AJ, Niebauer J, Lin PS, Tsao PS, Bernstein D & Cooke JP (2009). Hypercholesterolemia impairs exercise capacity in mice. *Vasc Med* **14,** 249–257.

Mayhan WG, Arrick DM, Patel KP & Sun H (2011). Exercise training normalizes impaired NOS-dependent responses of cerebral arterioles in type 1 diabetic rats. *Am J Physiol Heart Circ Physiol* **300,** H1013-1020.

Mayhan WG, Arrick DM, Sun H & Patel KP (2010). Exercise training restores impaired dilator responses of cerebral arterioles during chronic exposure to nicotine. *J Appl Physiol* **109,** 1109–1114.

Mihai G, He X, Zhang X, McCarthy B, Tran T, Pennell M, Blank J, Simonetti OP, Jackson RD & Raman SV (2011). Design and Rationale for the Study of Changes in Iron and Atherosclerosis Risk in Perimenopause. *J Clin Exp Cardiolog* **2,** 152.

Misko TP, Schilling RJ, Salvemini D, Moore WM & Currie MG (1993). A fluorometric assay for the measurement of nitrite in biological samples. *Anal Biochem* **214,** 11–16.

Moghadasian MH, McManus BM, Nguyen LB, Shefer S, Nadji M, Godin DV, Green TJ, Hill J, Yang Y, Scudamore CH & Frohlich JJ (2001). Pathophysiology of apolipoprotein E deficiency in mice: relevance to apo E-related disorders in humans. *FASEB J* **15,** 2623–2630.

Moraska A, Deak T, Spencer RL, Roth D & Fleshner M (2000). Treadmill running produces both positive and negative physiological adaptations in Sprague-Dawley rats. *Am J Physiol Regul Integr Comp Physiol* **279,** R1321-1329.

Nahrendorf M, Frantz S, Swirski FK, Mulder WJM, Randolph G, Ertl G, Ntziachristos V, Piek JJ, Stroes ES, Schwaiger M, Mann DL & Fayad ZA (2015). Imaging systemic inflammatory networks in ischemic heart disease. *J Am Coll Cardiol* **65,** 1583–1591.

Nichol KE, Poon WW, Parachikova AI, Cribbs DH, Glabe CG & Cotman CW (2008). Exercise alters the immune profile in Tg2576 Alzheimer mice toward a response coincident with improved cognitive performance and decreased amyloid. *J Neuroinflammation* **5,** 13.

Niebauer J, Maxwell AJ, Lin PS, Tsao PS, Kosek J, Bernstein D & Cooke JP (1999). Impaired aerobic capacity in hypercholesterolemic mice: partial reversal by exercise training. *Am J Physiol* **276,** H1346-1354.

Nighoghossian N, Wiart M, Cakmak S, Berthezène Y, Derex L, Cho T-H, Nemoz C, Chapuis F, Tisserand G-L, Pialat J-B, Trouillas P, Froment J-C & Hermier M (2007). Inflammatory response after ischemic stroke: a USPIO-enhanced MRI study in patients. *Stroke* **38,** 303–307.

Niki E (2009). Lipid peroxidation: physiological levels and dual biological effects. *Free Radic Biol Med* **47,** 469–484.

Oberley L & Spitz D (1985). Nitroblue tetrazolium. In *Handbook of methods for oxygen radical research*. CRC Press, Boca Raton.

Ohkawa H, Ohishi N & Yagi K (1979). Assay for lipid peroxides in animal tissues by thiobarbituric acid reaction. *Anal Biochem* **95,** 351–358.

Paglia DE & Valentine WN (1967). Studies on the quantitative and qualitative characterization of erythrocyte glutathione peroxidase. *J Lab Clin Med* **70,** 158–169.

Pedersen BK (2006). The anti-inflammatory effect of exercise: its role in diabetes and cardiovascular disease control. *Essays Biochem* **42,** 105–117.

Pellegrin M, Alonso F, Aubert J-F, Bouzourene K, Braunersreuther V, Mach F, Haefliger J-A, Hayoz D, Berthelot A, Nussberger J, Laurant P & Mazzolai L (2009*a*). Swimming prevents vulnerable atherosclerotic plaque development in hypertensive 2-kidney, 1-clip mice by modulating angiotensin II type 1 receptor expression independently from hemodynamic changes. *Hypertension* **53,** 782–789.

Pellegrin M, Miguet-Alfonsi C, Bouzourene K, Aubert J-F, Deckert V, Berthelot A, Mazzolai L & Laurant P (2009*b*). Long-term exercise stabilizes atherosclerotic plaque in ApoE knockout mice. *Med Sci Sports Exerc* **41,** 2128–2135.

Phinikaridou A, Andia ME, Protti A, Indermuehle A, Shah A, Smith A, Warley A & Botnar RM (2012). Noninvasive magnetic resonance imaging evaluation of endothelial permeability in murine atherosclerosis using an albumin-binding contrast agent. *Circulation* **126,** 707–719.

Pialoux V, Brown AD, Leigh R, Friedenreich CM & Poulin MJ (2009*a*). Effect of cardiorespiratory fitness on vascular regulation and oxidative stress in postmenopausal women. *Hypertension* **54,** 1014–1020.

Pialoux V, Mounier R, Brown AD, Steinback CD, Rawling JM & Poulin MJ (2009*b*). Relationship between oxidative stress and HIF-1 alpha mRNA during sustained hypoxia in humans. *Free Radic Biol Med* **46,** 321–326.

Podewils LJ, Guallar E, Kuller LH, Fried LP, Lopez OL, Carlson M & Lyketsos CG (2005). Physical activity, APOE genotype, and dementia risk: findings from the Cardiovascular Health Cognition Study. *Am J Epidemiol* **161,** 639–651.

Rowlatt C, Chesterman FC & Sheriff MU (1976). Lifespan, age changes and tumour incidence in an ageing C57BL mouse colony. *Lab Anim* **10,** 419–442.

Saleh A, Schroeter M, Jonkmanns C, Hartung H, Mödder U & Jander S (2004). In Vivo MRI of Brain Inflammation in Human Ischaemic Stroke. *Brain* **127,** 1670–1677.

Sexton WL (1995). Vascular adaptations in rat hindlimb skeletal muscle after voluntary running-wheel exercise. *J Appl Physiol* **79,** 287–296.

Shepherd D & Garland PB (1969). The kinetic properties of citrate synthase from rat liver mitochondria. *Biochem J* **114,** 597–610.

Shimada K, Kishimoto C, Okabe T, Hattori M, Murayama T, Yokode M & Kita T (2007). Exercise training reduces severity of atherosclerosis in apolipoprotein E knockout mice via nitric oxide. *Circ J* **71,** 1147–1151.

Sigovan M, Bessaad A, Alsaid H, Lancelot E, Corot C, Neyran B, Provost N, Majd Z, Breisse M & Canet-Soulas E (2010). Assessment of age modulated vascular inflammation in ApoE-/- mice by USPIO-enhanced magnetic resonance imaging. *Invest Radiol* **45,** 702–707.

Sigovan M, Kaye E, Lancelot E, Corot C, Provost N, Majd Z, Breisse M & Canet-Soulas E (2012). Anti-Inflammatory Drug Evaluation in ApoE-/- Mice by Ultrasmall Superparamagnetic Iron Oxide-Enhanced Magnetic Resonance Imaging. *Invest Radiol* **47,** 546–552.

Soto I, Graham LC, Richter HJ, Simeone SN, Radell JE, Grabowska W, Funkhouser WK, Howell MC & Howell GR (2015). APOE Stabilization by Exercise Prevents Aging Neurovascular Dysfunction and Complement Induction. *PLoS Biol* **13,** e1002279.

Stummer W, Weber K, Tranmer B, Baethmann A & Kempski O (1994). Reduced mortality and brain damage after locomotor activity in gerbil forebrain ischemia. *Stroke* **25,** 1862–1869.

Szostak J & Laurant P (2011). The forgotten face of regular physical exercise: a "natural" anti-atherogenic activity. *Clin Sci* **121,** 91–106.

Viboolvorakul S & Patumraj S (2014). Exercise training could improve age-related changes in cerebral blood flow and capillary vascularity through the upregulation of VEGF and eNOS. *Biomed Res Int* **2014,** 230791.

Weuve J, Kang JH, Manson JE, Breteler MMB, Ware JH & Grodstein F (2004). Physical activity, including walking, and cognitive function in older women. *JAMA* **292,** 1454–1461.

Wiart M, Davoust N, Pialat J-B, et al. MRI Monitoring of Neuroinflammation in Mouse Focal Ischemia (2007). *Stroke* **38**, 131–137.

Witko-Sarsat V1, Friedlander M, Capeillère-Blandin C, Nguyen-Khoa T, Nguyen AT, Zingraff J, Jungers P, Descamps-Latscha B (1996). Advanced oxidation protein products as a novel marker of oxidative stress in uremia. *Kidney Int* **49**, 1304-1313.

Zlokovic BV (2008). The Blood-Brain Barrier in Health and Chronic Neurodegenerative Disorders. *Neuron* **57,** 178–201.

TABLES

Table 1: Visual lesion characteristics

Score	Pre-contrast Image	Post-contrast Image
1	No abnormality	No observable change from pre-contrast
2	Small lesions (pixel > 10) on ≤ 2 slices	Change in SNR and increase in dark region size from pre-contrast on ≤ 2 slices
3	> 2 slices or medium size lesion (10<pixels<20) on ≤ 2 slices	Medium change in SNR and increase in dark region size from pre-contrast on ≤ 2 slices
4	Large lesion (>20 pixels) on > 2 slices	Major change in SNR and increase in dark region size from pre-contrast on > 2 slices

SNR: Signal to noise ratio

Table 2: Number of mice at inclusion, that died spontaneously, that died during experimental procedures, excluded after dissection for large tumors and used for biological assessments.

	Y-ApoE-UT	O-ApoE-UT	O-ApoE-ExT	O-C57-UT	O-C57-ExT
Mice at inclusion (n)	20	53	38	8	8
Mice that died spontaneously (n)	0	29	10	1	1
Mice that died during ITT and MRI (n)	0	3	3	0	0
Mice excluded after dissection for large tumors (n)	0	2	1	0	0
Mice used for biological assessments (n)	20	19	24	7	7

ITT: insulin tolerance test; MRI: magnetic resonance imaging; Y-ApoE-UT: young adult ApoE$^{-/-}$ untrained; O-ApoE-UT: old ApoE$^{-/-}$ untrained; O-ApoE-ExT: old ApoE$^{-/-}$ exercise trained; O-C57-UT: old C57BL/6 untrained; O-C57-ExT: old C57BL/6 exercise trained.

Table 3: Effect of age and exercise training on body weight, citrate synthase activity, cholesterol and insulin resistance

	Y-ApoE-UT	O-ApoE-UT	O-ApoE-ExT	O-C57-UT	O-C57-ExT
Body weight (g)	32.7±1.5	40.2±1.5*	38.5±1.5*	27.2±1.2	27.7±1.1
Citrate Synthase (nmol/min/mg)	3.68±0.2	6.76±0.8*	8.50±0.2*†	4.92±0.42*	8.44±0.86*†
Cholesterol (mmol/L)	22.0±4.1	18.2±2.0	15.5±1.2*†	6.2±0.6#	5.0±0.4*#
Insulin Resistance (%)	-20.7±8.1	-11.6±2.2*	-22.3±2.8†	-24.9±2.4	-26.5±1.9

Insulin resistance was estimated as the % change of glycemia at 30min (*vs.* baseline) during insulin tolerance test. Y-ApoE-UT: young adult ApoE$^{-/-}$ untrained; O-ApoE-UT: old ApoE$^{-/-}$ untrained; O-ApoE-ExT: old ApoE$^{-/-}$ exercise trained; O-C57-UT: old C57BL/6 untrained; O-C57-ExT: old C57BL/6 exercise trained. * Significantly different from Young; † Significantly different from corresponding Untrained; # Significantly different from corresponding ApoE$^{-/-}$ $P<0.05$.

Table 4: Effect of age and exercise training on brain markers of inflammation and oxidative stress

	Y-ApoE-UT	O-ApoE-UT	O-ApoE-ExT	O-C57-UT	O-C57-ExT
MDA (µmol/mg)	3.8±0.6	9.1±1.4*	5.2±0.9*†	1.6±1.3#	0.7±0.3#
TNFα (pg/mg)	47.4±3.7	137.9±20.8*	114.1±8.9*†	36.6±4.0#	31.2±4.7#*
IL-1β (pg/mg)	127.7±18.7	226.8±27.1*	182.5±21.5*†	84.5±19.7#	88.3±13.2#
AOPP (µmol/mg)	14.5±1.1	16.1±1.4	12.7±1.2†	3.1±1.1#†	4.8±2.5#†
Catalase (µmol/min/mg)	174.1±14.6	65.5±6.3*	90.2±11.5*†	33.7±10.4#*	46.3.2±29.3#*
GPX (µmol/min/mg)	168.0±11.4	74.3±1.5*	74.7±12.0*	77.0±13.9*	73.9±10.1*
FRAP (µmol/mg)	62.2±4.1	56.9±5.2	50.7±4.3	70.1±15.3#*	65.4±29.4
SOD (µmol/min/mg)	9.56±0.8	6.96±1.1*	7.16±0.9*	7.39±3.20	6.33±2.55*

MDA: lipid peroxidation; TNFα: tumor necrosis factor alpha; IL-1β: Interleukin 1β; AOPP: protein oxidation; GPX, catalase and SOD: antioxidant enzymes activities; FRAP: ferric reducing antioxidant power. Y-ApoE-UT: young adult $ApoE^{-/-}$ untrained; O-ApoE-UT: old $ApoE^{-/-}$ untrained; O-ApoE-ExT: old $ApoE^{-/-}$ exercise trained; O-C57-UT: old C57BL/6 untrained; O-C57-ExT: old C57BL/6 exercise trained. * Significantly different from Young; † Significantly different from corresponding Untrained; # Significantly different from corresponding $ApoE^{-/-}$ $P<0.05$.

Table 5: Effect of age and exercise training on aorta TNFa, IL-1β, AOPP and SOD

	Y-ApoE-UT	O-ApoE-UT	O-ApoE-ExT	O-C57-UT	O-C57-ExT
TNFα (pg/mg)	6.7±1.7	11.8±1.2*	9.6±1.5*†	0.5±0.3	2.5±1.3
IL-1β (pg/mg)	16.7±4.9	47.8±17.6*	28.0±10.7*†	0.9±0.2#	1.0±0.2#
AOPP (µmol/mg)	21.6±1.4	159.5±25.2*	122.3±20.9*†	8.4±2.7#	9.1±2.9#
SOD (µmol/min/mg)	9.27±2.1	26.2±1.7*	6.7±2.0†	7.79±1.7#	5.59±1.8

TNFα: tumor necrosis factor alpha; IL-1β: Interleukin 1β; AOPP: protein oxidation; SOD: superoxide dismutase activity. Y-ApoE-UT: young adult $ApoE^{-/-}$ untrained; O-ApoE-UT: old $ApoE^{-/-}$ untrained; O-ApoE-ExT: old $ApoE^{-/-}$ exercise trained; O-C57-UT: old C57BL/6 untrained; O-C57-ExT: old C57BL/6 exercise trained. * Significantly different from Young; † Significantly different from corresponding Untrained; # Significantly different from corresponding $ApoE^{-/-}$ $P<0.05$.

Table 6: Effect of age and exercise training on heart and liver markers of oxidative stress and antioxidants

	Y-ApoE-UT	O-ApoE-UT	O-ApoE-ExT	O-C57-UT	O-C57-ExT
AOPP-heart (µmol/mg)	28.5±2.4	75.3±5.8*	68.4±5.6*†	152.7±14.4#	138.9±6.1#
Catalase-heart (µmol/min/mg)	831±76	2492±436*	2033±400*†	4955±508#	4266±449#
GPX-heart (µmol/min/mg)	451±11	322.7±7*	338±7*	834±87#	781±83#
SOD-heart (µmol/min/mg)	32.7±4.5	24.1±2.8*	32.2±2.4†	48.0±6.6#	44.9±7.9#
AOPP-liver (µmol/mg)	14.8±5.3	41.4±10.9*	36.0±9.1*†	6.6±2.0#	9.3±3.4#
MDA-liver (µmol/mg)	0.75±0.42	4.11±2.08*	2.37±1.42*†	1.87±0.45#	2.37±1.47
SOD-liver µmol/min /mg)	0.92±0.12	0.71±0.26	0.83±0.13†	0.75±0.24	0.79±0.21
GPX-liver µmol/min/mg)	14.8±12.9	6.0±4.5*	27.4±9.6*†	10.9±1.5	22.7±6.6

AOPP: protein oxidation; GPX, catalase and SOD: antioxidant enzymes activities; FRAP: ferric reducing antioxidant power. Y-ApoE-UT: young adult $ApoE^{-/-}$ untrained; O-ApoE-UT: old $ApoE^{-/-}$ untrained; O-ApoE-ExT: old $ApoE^{-/-}$ exercise trained; O-C57-UT: old C57BL/6 untrained; O-C57-ExT: old C57BL/6 exercise trained. * Significantly different from Young; † Significantly different from corresponding Untrained; # Significantly different from corresponding $ApoE^{-/-}$ $P<0.05$.

Table 7: Effect of age and exercise training on plasma markers of oxidative stress, antioxidants and inflammation

	Y-ApoE-UT	O-ApoE-UT	O-ApoE-ExT	O-C57-UT	O-C57-ExT
AOPP (µmol/L)	202.6±9.1	152.4±11.8*	131.0±10.7*	15.3±2.6#	13.3±2.7#
GPX (µmol/L/min)	123.0±17.7	113.4±14.5	102.4±13.7	109.3±15.2	227.0±62.8†
Nitrotyrosine (nmol/L)	25.6±3.8	50.6±11.0*	66.4±8.9*	36.4±4.0#	26.4±5.2#
NOx (µmol/L)	22.3±1.3	22.6±1.0	27.3±1.1*†	28.3±2.4#	35.7±3.2*†#
SOD (µmol/mL/min)	37.1±1.0	32.3±1.4*	36.7±1.2	27.3±1.8	33.3±3.1†
TNFα (pg/mL)	82.3±7.9	42.3±8.9*	40.8±6.7*	46.3±5.6	72.4±16.4†
IL-1β (pg/mL)	157.6±14.7	118.2±6.8*	114.2±8.2*	111.5±22.7	105.4±12.8

AOPP: protein oxidation; Nitrotyrosine: protein nitration; GPX and SOD: antioxidant enzymes activities; NOx: nitric oxide metabolism (nitrites + nitrates); FRAP: ferric reducing antioxidant power; TNFα: tumor necrosis factor alpha; IL-1β: Interleukin 1β. Y-ApoE-UT: young adult $ApoE^{-/-}$ untrained; O-ApoE-UT: old $ApoE^{-/-}$ untrained; O-ApoE-ExT: old $ApoE^{-/-}$ exercise trained; O-C57-UT: old C57BL/6 untrained; O-C57-ExT: old C57BL/6 exercise trained. * Significantly different from Young; † Significantly different from corresponding Untrained; # Significantly different from corresponding $ApoE^{-/-}$ $P<0.05$.

Table 8: Correlations between brain markers of oxidative stress and inflammation in young and old ApoE mice

Variables	-with	N	Pearson's Correlation	p-value
MDA-brain	IL-1β-brain	26	.429	0.029
AOPP-brain	IL-1β-brain	26	.764	0.000
Catalase-brain	FRAP-brain	27	.453	0.018
	SOD-brain	27	.573	0.002
	GPX-brain	26	.505	0.009
TNFα-brain	IL-1β brain	27	.508	0.007
FRAP-brain	SOD-brain	27	.552	0.003
	GPX-brain	26	.515	0.007
SOD-brain	GPX-brain	26	.683	0.000

Table 9: Lack of correlations between brain and plasma markers of oxidative stress and inflammation

Variables	-with	N	Pearson's Correlation	p-value
TNFα-plasma	TNFα-brain	21	-.1818	0.430
IL-1β-plasma	IL-1β-brain	22	.1700	0.449
AOPP-plasma	AOPP-brain	42	.1482	0.349
MDA-plasma	MDA-brain	27	-.0811	0.688
SOD-plasma	SOD-brain	27	.1836	0.359

FIGURES

Fig. 1: MR imaging protocol. A pre-contrast imaging (T-0h) protocol was performed on the aorta followed immediately by brain imaging with gadolinium injection. An ultrasmall iron oxide nanoparticles (USPIO) contrast agent, P904 (Guerbet, France), was then injected. 48 hours later (T-48h), an identical post-USPIO aorta imaging protocol was performed for inflammation assessment. This was immediately followed by brain inflammation imaging.

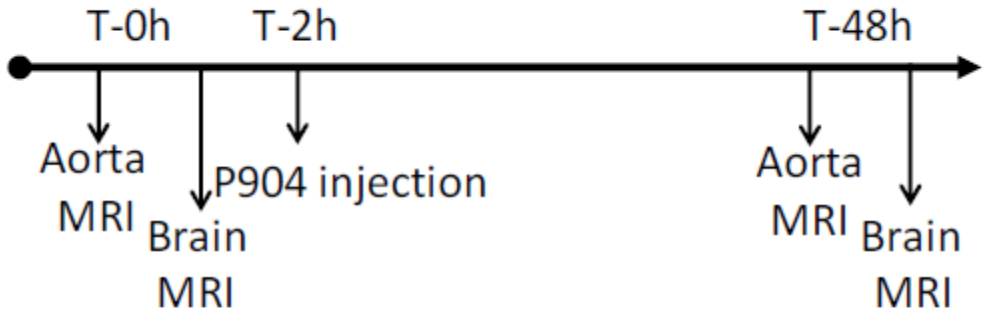

Figure 1

Fig. 2: Survival Rate for old untrained (O-ApoE-UT) and exercise trained (O-ApoE-ExT) ApoE$^{-/-}$ mice (p=0.03);

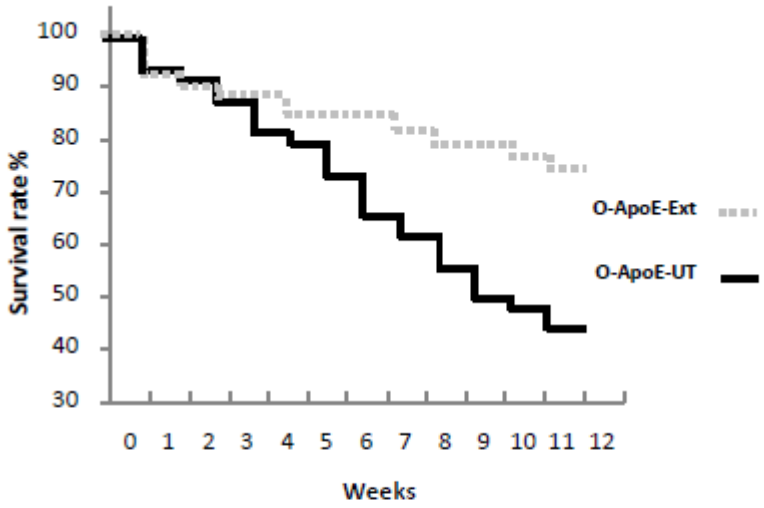

Figure 2

Fig.3

(A): Brain MRI in old untrained ApoE$^{-/-}$ (O-ApoE-UT, left) versus old untrained C57 (O-C57-UT, right) (pre-USPIO T2 MRI, i to ii; and 48h-post-USPIO T2 MRI, iii to iv; post-gadolinium T1 MRI, v to vi). In O-ApoE-UT mice, red arrows show a hypointense region suggesting inflammation in panels i. and iii. and bright zone in panel v. suggesting BBB leakage.

(B): Brain T2 MRI (pre-USPIO, i to ii, and 48h-post-USPIO, iii to iv) in untrained (O-ApoE-UT, left) versus trained old ApoE$^{-/-}$ mice (O-ApoE-Ext, right) showing a hypointense region (red arrow, iii) demonstrating inflammation in the left periventricular fornix fimbria in the O-ApoE-UT mouse, and a normal image in the O-ApoE-ExT (iv).

(C): Brain pre and post-USPIO T2* Scores and post-gadolinium T1 Score for old sedentary and trained ApoE$^{-/-}$ mice (O-ApoE-UT; O-ApoE-Ext) and old sedentary and trained C57 mice (O-C57-UT; O-C57-Ext). * Significantly different O-ApoE-ExT vs. O-ApoE-UT; † Significantly different from O-C57-UT vs. O-ApoE-UT $P<0.05$. ‡ Significantly different from Pre-Contrast $P<0.05$.

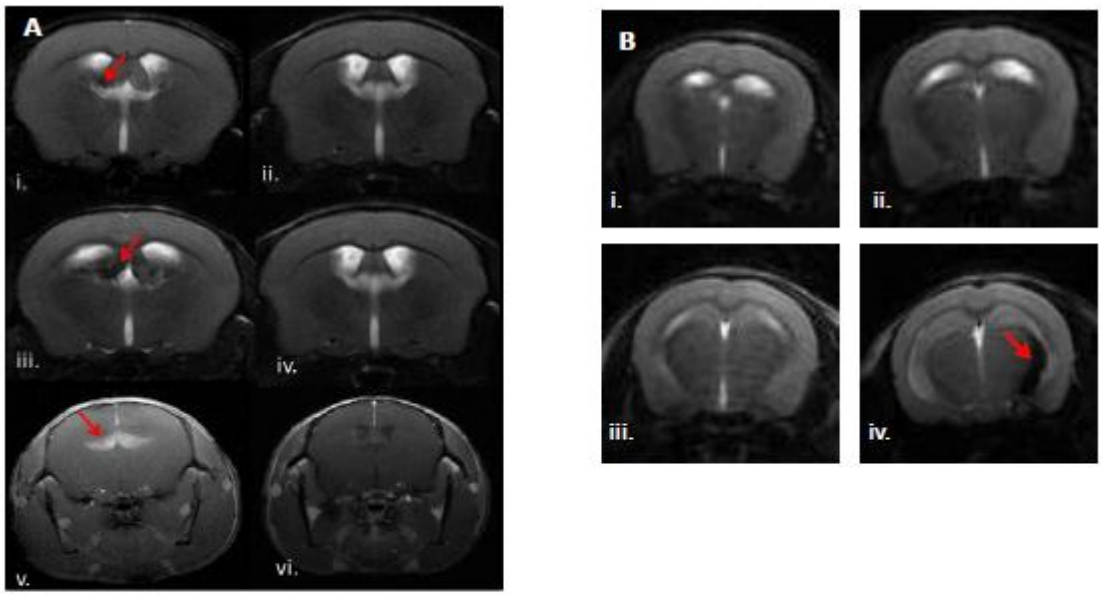

C	O-ApoE-UT	O-ApoE-ExT	O-C57-UT	O-C57-ExT
T2* Pre-Contrast Score	1.71±0.2	1.29±0.2	1.44±0.2	1.30±0.3
T2* Post-Contrast Score	2.92±0.5‡†	1.69±0.4‡*	1.50±0.2	1.43±0.2
Gadolinium Score	2.70±0.8†	N/A	1.42±0.3	1.36±0.2

Figure 3

Fig. 4: Brain MR images of an old untrained ApoE$^{-/-}$ mouse. Pre (A) and post-USPIO (B) T2 images both showing hyposignal and heterogenous regions around the choroid plexus representative of vascular sequelae (A, arrow) and inflammation (B, arrow); Pre (C) and post-USPIO (D) T2* maps, with an increase of the hyposignal region on post-USPIO, suggesting iron deposits (C, arrow) and phagocytic activity (D, arrow); Pre (E) and post-gadolinium (F) T1 images, the enhancing bright zone showing BBB leakage in the same area (F); Positive F4/80 staining confirming macrophages in this area (G); Positive IgG staining (H) in the same locations confirming MRI findings of BBB leakage.

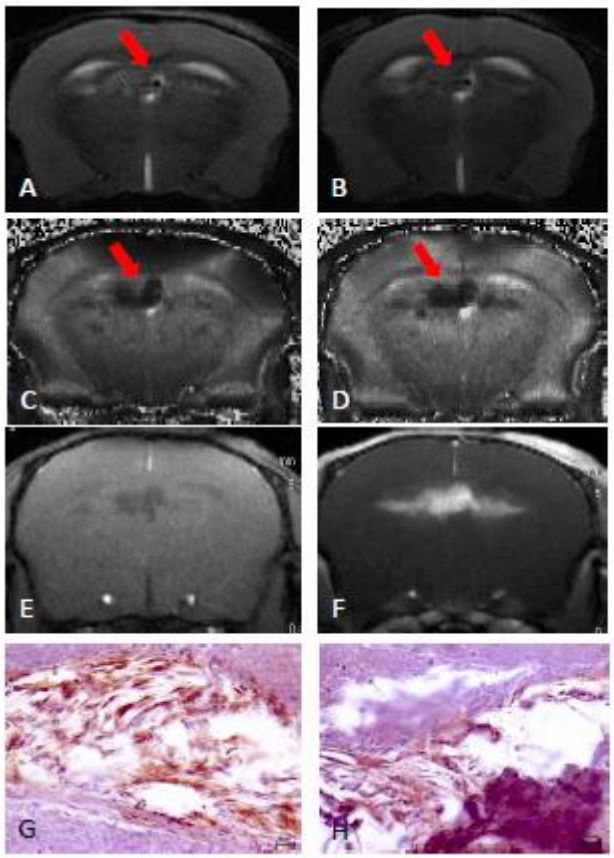

Figure 4

Fig. 5: Pre- and post-USPIO T2* maps of the ascending aorta in a young untrained (Y-ApoE-UT), an old untrained (O-ApoE-UT) and an old trained (O-ApoE-Ext) ApoE$^{-/-}$ mouse (A). Ascending aorta vessel wall area measurements (B), and vessel wall pre and post-USPIO T2* measurements (C). In O-ApoE-UT, vessel wall area is significantly larger, and pre and post-USPIO T2* significantly lower, representative of advanced and complex atherosclerotic lesions with inflammatory activity. * Significantly different from old ApoE mice (O-ApoE-UT); † Significantly different from young ApoE mice (Y-ApoE-UT); ‡ Significantly different from Pre-Contrast. $P < 0.05$

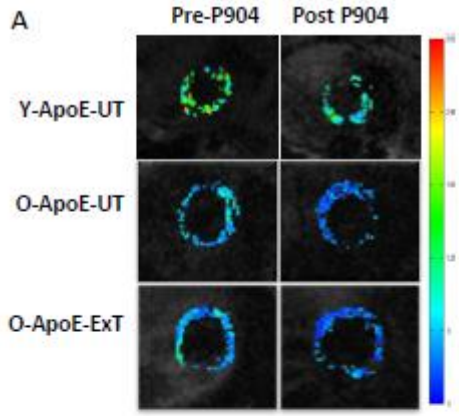

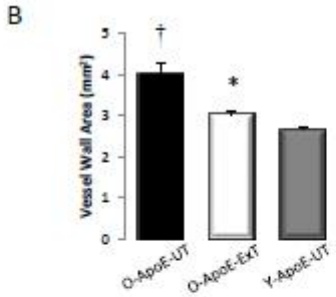

C	Y-ApoE-UT	O-ApoE-UT	O-ApoE-ExT
T2* Pre-Contrast	12.3±0.1	10.9±0.1*	11.5±0.1*†
T2* Post-Contrast	9.9±0.1‡	8.1±0.1*‡	8.7±0.1*†‡

Figure 5

Fig. 6: (A) negative control, (B) positive F4/80 and (C) positive IgG for an old ApoE untrained mouse (left side, at the level of the Fornix Fimbriae, x20). (D) negative control, (E) positive F4/80 and (F) positive IgG for an old C57 untrained mouse (left side, at the level of the Fornix Fimbriae, x20).

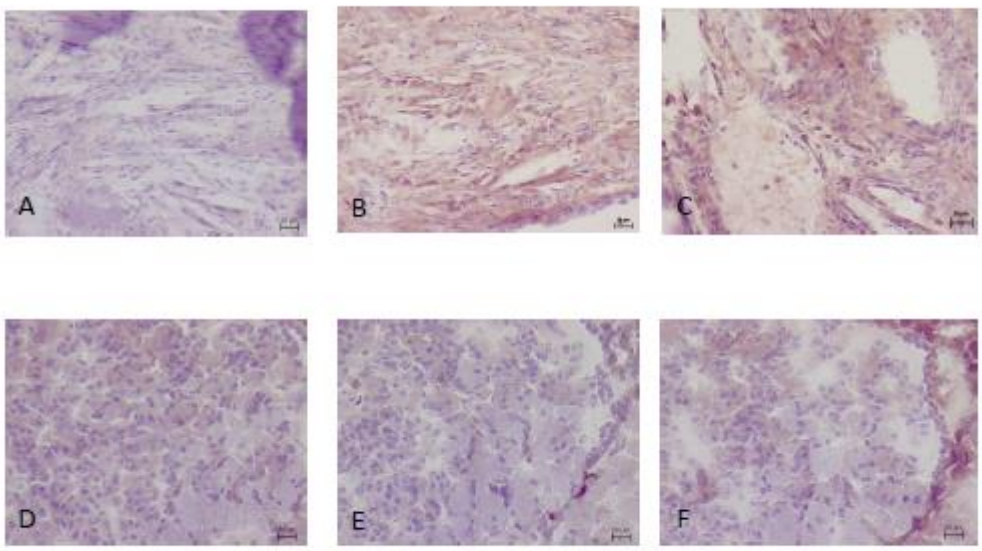

Figure 6